



HHS Public Access

Author manuscript

J Appl Toxicol. Author manuscript; available in PMC 2016 July 01.

Published in final edited form as:

J Appl Toxicol. 2016 April ; 36(4): 618–626. doi:10.1002/jat.3253.

Pulmonary toxicity of indium-tin oxide production facility particles in rats

Melissa A. Badding^{a,*}, Natalie R. Fix^a, Marlene S. Orandle^a, Mark W. Barger^a, Katherine M. Dunnick^a, Kristin J. Cummings^b, and Stephen S. Leonard^a

^aHealth Effects Laboratory Division, National Institute for Occupational Safety and Health, Morgantown, WV, 26505, USA

^bDivision of Respiratory Disease Studies, National Institute for Occupational Safety and Health, Morgantown, WV, 26505, USA

Abstract

Indium-tin oxide (ITO) is used to make transparent conductive coatings for touch-screen and liquid crystal display electronics. Occupational exposures to potentially toxic particles generated during ITO production have increased in recent years as the demand for consumer electronics continues to rise. Previous studies have demonstrated cytotoxicity *in vitro* and animal models have shown pulmonary inflammation and injury in response to various indium-containing particles. In humans, pulmonary alveolar proteinosis (PAP) and fibrotic interstitial lung disease have been observed in ITO facility workers. However, which indium materials or specific processes in the workplace may be the most toxic to workers is unknown. Here we examined the pulmonary toxicity of three different particle samples that represent real-life worker exposures, as they were collected at various production stages throughout an ITO facility. Indium oxide (In₂O₃), sintered ITO (SITO) and ventilation dust (VD) particles each caused pulmonary inflammation and damage in rats over a time course (1, 7 and 90 days post-intratracheal instillation), but SITO and VD appeared to induce greater toxicity in rat lungs than In₂O₃ at a dose of 1 mg per rat. Downstream pathological changes such as PAP and fibrosis were observed in response to all three particles 90 days after treatment, with a trend towards greatest severity in animals exposed to VD when comparing animals that received the same dose. These findings may inform workplace exposure reduction efforts and provide a better understanding of the pathogenesis of an emerging occupational health issue. Published 2015. This article is a U.S. Government work and is in the public domain in the USA.

Keywords

indium-tin oxide; occupational exposure; pulmonary toxicity; cytokines; phagocytosis

*Correspondence to: Melissa A Badding, Center for Toxicology and Mechanistic Biology, Exponent, Alexandria, VA, 22314, USA, mbadding@exponent.com.

Disclaimer

The findings and conclusions in this report are those of the authors and do not necessarily represent the views of the National Institute for Occupational Safety and Health.

Conflict of interest

The Authors did not report any conflict of interest.

Introduction

Indium-tin oxide (ITO) is used as a transparent conductive coating in the manufacture of electronics such as touch-screen phones, liquid crystal displays (LCD) and solar panels. To achieve the final product, an ITO tile that can be used to make 'thin film' coatings, indium oxide (In_2O_3) and tin oxide (SnO_2) are mixed in a 90:10 ratio (wt:wt) and fired at high temperatures to sinter the ITO mixture into a solidified tile (Udawatte and Yanagisawa, 2001; Kim *et al.*, 2002). Recently, the demand for ITO has increased as the production of consumer electronics continues to expand.

The expansion of the ITO industry has resulted in the emergence of indium lung disease, an occupational illness that has affected workers exposed to indium-containing compounds. Cases of lung disease in indium-exposed workers began to be reported in the medical literature in 2003 (Homma *et al.*, 2003; Cummings *et al.*, 2012). In terms of pulmonary symptoms and signs, workers exposed to indium-containing particles by inhalation develop a cough, dyspnea, and abnormalities on pulmonary function tests and chest computed tomography (CT) scans (Homma *et al.*, 2003; Omae *et al.*, 2011; Cummings *et al.*, 2012). Epidemiologic investigation in plants with cases of indium lung disease have demonstrated elevated serum biomarkers of interstitial lung disease and functional and radiographic abnormalities in co-workers (Chonan *et al.*, 2007; Hamaguchi *et al.*, 2008; Nakano *et al.*, 2009; Cummings *et al.*, 2013; Cummings *et al.*, 2014).

A recent comprehensive clinical analysis of 10 reported cases, including two from an ITO production facility in the United States, demonstrated that workers presented with pulmonary alveolar proteinosis (PAP) (within 6–14 months of starting work) or fibrotic interstitial lung disease with or without emphysema (within 2–14 years of starting work) (Cummings *et al.*, 2012). The current study and our previous studies (Badding *et al.*, 2014b; Badding *et al.*, 2015) have utilized particles collected from this same US facility at various stages in the ITO production process. These samples are in the micron size range and include In_2O_3 , particles generated during the grinding of sintered ITO (SITO) tiles, and dusts generated during the reclamation of indium from production waste materials and spent tiles (ventilation dust). Thus, we were able to expose rats to the same particles that workers may encounter throughout the ITO production process.

Previous studies of indium-containing particles have demonstrated toxicity *in vitro* (Lison *et al.*, 2009; Gwinn *et al.*, 2013; Badding *et al.*, 2014b; Badding *et al.*, 2015) and pulmonary inflammation in rodent models (Lison *et al.*, 2009; Tanaka *et al.*, 2010; Nagano *et al.*, 2011a, b; Lim *et al.*, 2014; Gwinn *et al.*, 2015). Rat and mouse studies of ITO intratracheal instillation or inhalation demonstrated significant pulmonary changes, including inflammatory cell infiltrates, alveolar proteinosis and interstitial fibrosis (Tanaka *et al.*, 2010; Nagano *et al.*, 2011a, b). In some studies, ITO was shown to be more toxic and induce more lung damage than In_2O_3 (Lison *et al.*, 2009; Nagano *et al.*, 2011a, b). However, indium phosphide particles, which are composed of indium that is relatively more soluble than indium found in ITO, were shown to be more toxic than ITO in one study (Gwinn *et al.*, 2015).

In vitro studies from our lab and others suggest that macrophages play a role in the toxicity of indium-containing particles and that pulmonary epithelial cells are also sensitive to these exposures. Our recent findings suggest that both cell types have proinflammatory responses when exposed to SITO particles (Badding *et al.*, 2015). Additionally, we found that macrophage uptake of SITO or dust collected from the ventilation system in the indium reclamation department of the facility (ventilation dust) impaired subsequent phagocytosis of *Escherichia coli*, implicating macrophage dysfunction from these exposures (Badding *et al.*, 2015).

The main goal of this study was to determine the adverse pulmonary effects of various respirable particles found in an ITO production facility. Given that the particles were collected from the starting materials, ITO grinding, and indium reclaim departments, we wanted to determine whether a particular stage or process puts workers at higher risk for developing indium lung disease. Our findings suggest that all three particle types cause proinflammatory responses and lung damage to varying degrees, but that dust from the reclaim department (ventilation dust) may be the most hazardous to workers.

Materials and methods

ITO production particles

The particles used in this study were collected at a United States ITO production facility from containers of feedstock materials or production processes (NIOSH, 2012). Indium oxide (In_2O_3) is from the refinery, sintered ITO (SITO) is from the ITO department's grinding area; and ventilation dust (VD) is from the reclamation department where indium metal is reclaimed from waste materials. The particles have been previously characterized and evaluated for toxicity *in vitro* (Badding *et al.*, 2014b). SITO had been in contact with metalworking fluid and was found to have low levels of endotoxin present, but was still found to be cytotoxic when endotoxin activity was removed with heat (Badding *et al.*, 2015). The In_2O_3 is crystallographically pure and the other two samples are mixtures. SITO is 44% O, 19% C, 24% In, and 2.7% Sn, and VD is 21% O, 49% C, 12% In, and 0% Sn (atom % at particle surface by X-ray photoelectron spectroscopy). The mean aerodynamic diameters are $2.7 \pm 2.2 \mu\text{m}$ for In_2O_3 , $1.2 \pm 0.8 \mu\text{m}$ for SITO and $0.5 \pm 0.3 \mu\text{m}$ for VD (Badding *et al.*, 2014b).

Animals

Male Sprague–Dawley [Hla:(SD) CVF] rats from Hilltop Lab Animals (Scottsdale, PA, USA), weighing 270–330 g were used for all exposures. Animals were acclimated for at least 7 days after arrival and housed under a standard 12-h day/night cycle at 20–25 °C. They were provided HEPA-filtered air, irradiated Teklad 2918 diet and tap water *ad libitum*. Animal facilities are specific pathogen-free, environmentally controlled and accredited by the Association for Assessment and Accreditation of Laboratory Animal Care International (AAALAC). All animal procedures used in the study were reviewed and approved by the NIOSH Animal Care and Use Committee.

Intratracheal particle instillation

The particles were suspended in sterile, endotoxin- and Ca^{2+} , Mg^{2+} -free phosphate-buffered saline (PBS), pH 7.4. Rats were lightly anesthetized by an intraperitoneal injection of 30–40 mg kg^{-1} body weight sodium methohexital (Brevital, Eli Lilly, Indianapolis, IN, USA) and intratracheally instilled with 1.0 and 5.0 mg rat^{-1} In_2O_3 or SITO in 300 μl of sterile PBS. For VD, rats received 0.5 and 1.0 mg rat^{-1} owing to the mortality at 5.0 mg rat^{-1} . For each condition (particle sample and time point), animals were intratracheally instilled with 300 μl of sterile PBS as vehicle controls (0 mg). Dosages were determined using the recommended exposure limit (REL) for Indium (0.1 mg m^{-3}), ventilation rate ($9.6 \text{ m}^3 \text{ day}^{-1}$) and deposition fraction (0.2). For lung burdens of 0.5, 1 and 5 mg, it would take 2.5, 5 and 25 work years ($260 \text{ days year}^{-1}$), respectively, to reach those amounts (considering normalization for rat body weights and lung surface area).

Bronchoalveolar lavage

At 1, 7 and 90 days post-intratracheal instillation (IT), bronchoalveolar lavage (BAL) was performed. Animals were euthanized with an intraperitoneal injection of sodium pentobarbital ($>100 \text{ mg kg}^{-1}$ body weight; Sleepaway, Fort Dodge Animal Health, Wyeth, Madison, NJ, USA) and exsanguination. A tracheal cannula was inserted, and the lungs were lavaged with 6 ml of ice-cold endotoxin- and Ca^{2+} , Mg^{2+} -free PBS (pH 7.4). The recovered BAL fluid (BALF) was centrifuged at 650 g for 10 min at 4 °C, and the resultant cell-free supernatant was transferred to tubes for analysis of lung injury and inflammatory parameters. The cell pellets from each rat were resuspended in 1 ml of PBS and evaluated as described below.

Evaluation of cells and lung injury from BALF

The total cell numbers, alveolar macrophages and polymorphonuclear leukocytes (PMNs) recovered by BAL were determined using a Beckman Coulter Multisizer 4 Analyzer (Beckman Coulter Indianapolis, IN, USA). Cells were differentiated using a Cytospin 3 centrifuge (Shandon Life Sciences International, Cheshire, England). Cell suspensions (1×10^5 cells) were spun for 5 min at $72 \times g$ and pelleted onto a slide. The cytopsin preparations were stained with modified Wright–Giemsa stain, and cell differentials were determined by light microscopy. Differential cell counts were calculated by multiplying the total cell counts (~ 200 per rat) by the cell differential percentage obtained from the cytopsin preparations. Using the acellular fraction of BALF, lactate dehydrogenase (LDH) activity, an indicator of general cell damage and toxicity, was measured. LDH activity was determined by measuring the oxidation of lactate to pyruvate coupled with the formation of NADH at 340 nm. Measurements were performed with a COBAS C111 auto-analyzer (Roche Diagnostics USA, Indianapolis, IN, USA).

Phagocytosis assay

After counts from BALF, the cell suspensions were centrifuged again, and pellets were resuspended at the desired macrophage concentration of $1 \times 10^6 \text{ cells ml}^{-1}$ in minimal essential medium (MEM) with Eagle's salts, 10% fetal bovine serum and 50 mg ml^{-1} penicillin/streptomycin (Invitrogen Life Sciences, Grand Island, NY, USA). Cells were then

plated at 2.5×10^5 macrophages per well in 96-well dishes and incubated at 37 °C in a 5% CO₂ incubator for 1 h to allow attachment. Cells were washed three times with medium to remove the unattached (and non-phagocytic) cells. A previous study by our group demonstrated that plated cells recovered from rat BAL are predominantly macrophages, even after silica particle treatments (Antonini *et al.*, 2000). Therefore, the remaining adherent cells used in the assay were mostly macrophages, although small amounts of other phagocytes (PMNs) may have been attached as well.

The pHrodo™ Red *E. coli* BioParticles® were prepared according to manufacturer's instructions (Molecular Probes, Carlsbad, CA, USA), and the assay was carried out as previously described (Badding *et al.*, 2014a). These particles allow specific detection of phagocytosed particles versus adherent and extracellular particles, as a result of the pH-sensitive fluorogenic dye. Briefly, wells were washed again prior to the addition of BioParticle suspensions to all wells, including blanks (no cells) to be subtracted from all experimental wells. After incubation for 2 h at 37 °C, plates were read at 560 nm excitation/600 nm emission to measure changes in fluorescence. All conditions were run in triplicate wells and macrophages from at least four rats per condition were used. Cytochalasin D (Sigma-Aldrich, St. Louis, MO, USA) at a final concentration of 10 µM was used as a positive control to inhibit phagocytosis in a second set of wells containing macrophages from PBS vehicle control-treated rats. The percentage of maximal phagocytosis was calculated as a ratio of the net experimental phagocytosis to the phagocytosis by the PBS control group (0 mg).

Enzyme-linked immunosorbent assay (ELISA)

BALF from each rat was frozen at -80 °C. Cytokine levels were measured with ELISA kits (rat IL-6; cat. no. ER3IL65, rat IL-1β; cat. no. ER2IL1B, rat TNF-α; cat. no. ER3TNFA; Thermo Scientific, Rockford, IL, USA) according to manufacturer's instructions. All conditions were run in duplicate wells.

Plasma indium determination

Whole blood was collected for indium content analysis via the abdominal aorta into BD Vacutainer tubes (cat. no. 368381, K2 EDTA plastic royal blue top; BD, Franklin Lakes, NJ, USA), which led to exsanguination after sodium pentobarbital injection. Blood tubes were immediately placed on a rocker for 10 min, followed by centrifugation for 10 min using a refrigerated centrifuge (Sorvall Legend XTR). The resulting plasma supernatant was immediately transferred to a clean polypropylene tube using a Pasteur pipette. The samples were frozen at -80 °C, then shipped on dry ice to NMS Labs (Willow Grove, PA, USA) for plasma indium analysis using inductively coupled plasma mass spectrometry (ICP-MS) with a 0.03 mcg l⁻¹ limit of detection.

Histopathological analysis

At 90 days post-exposure, formalin-fixed sections of lung from 35 animals were stained with Hematoxylin and eosin (H&E) and Picosirius Red and evaluated microscopically for evidence of inflammation, alveolar proteinosis and interstitial fibrosis. The left lung was examined for each animal. To follow diagnostic terminology and procedures used in

previous studies (Shackelford *et al.*, 2002; Mann *et al.*, 2012), each microscopic change was scored for severity according to the following parameters: 1 = minimal, 2 = mild, 3 = moderate, 4 = moderately severe, and 5 = severe. Statistical analysis was not performed owing to the small numbers of animals used for each group ($n = 3-5$).

Statistical analysis

All data are represented as the mean \pm SEM for each condition. One-way and two-way analysis of variance tests with Tukey or Dunnett's post-tests were performed using GraphPad Prism 6 software (GraphPad Software, Inc., La Jolla, CA, USA) for each experiment to compare the responses between groups, and statistical significance is shown when $P < 0.05$.

Results

Parameters of bronchoalveolar lavage

The instilled particles used in this study included one of the starting materials (In_2O_3), particles generated during grinding and cutting of sintered ITO tiles (SITO), and ventilation dust (VD) collected from the indium reclaim department, which also contains SITO as well as other forms of indium (Badding *et al.*, 2014b). These samples represent potential particle exposures in different parts of the facility. To evaluate pulmonary damage and inflammation in the lungs of rats after intratracheal instillation (IT) of these particles, bronchoalveolar lavage (BAL) was performed. The BAL fluid (BALF) analyzes indicate that each particle type induced pulmonary toxicity, but to varying degrees and with differing amounts of cell infiltration and pulmonary damage (Fig. 1). The higher doses of SITO and VD were associated with the greatest LDH values on day 7 post-IT (Fig. 1A). This was dramatically reduced by day 90 in the BALF of VD-treated rats, but persisted in SITO-treated rat BALF and continued to rise in 1 mg-treated SITO rats.

Cell counts from SITO-treated rat lungs at both doses drastically increased from day 1 to 7 and continued through day 90 post-treatment (Fig. 1B). In_2O_3 treatment induced a similar trend of increasing cell counts, but at much lower levels than with SITO treatment. In fact, only the 5-mg dose of In_2O_3 caused significant changes in the BALF parameters measured over PBS vehicle control rats, but the counts were still lower than those from 1 mg SITO-treated rats. Treatment with VD also resulted in significantly elevated cell counts, but the number of recovered cells was reduced in the day 90 BALF. It is important to note that at day 7, 1-mg VD and 5-mg SITO induced similar levels of LDH and cell counts recovered from BAL.

Cell differential analysis demonstrated that cells in rat lungs were mostly PMNs and macrophages following treatments with all three particle samples (Fig. 2). The results for each particle type appear very similar between days 1 and 7, with shifts in cell percentages (from predominantly PMNs to macrophages) occurring at day 90 for In_2O_3 and VD (Fig. 2C). However, cells from SITO-exposed rats maintained very similar cell differentials by day 90 (still mainly PMNs). In contrast, 1-mg In_2O_3 treatment caused a much lower percentage of PMN infiltrates compared with 1-mg SITO or VD, and BALF from the 5-mg

In₂O₃ exposure had a lower percentage of PMNs compared with 5-mg SITO at all time-points.

Cytokine production

Cytokines measured from cell-free BALF show a proinflammatory response in the lungs of treated rats (Fig. 3). TNF- α was only significantly elevated with SITO treatment at day 1 post-IT with the 5-mg dose, whereas IL-6 and IL-1 β were elevated with various treatments and at multiple time points. IL-6 was not induced by In₂O₃ under any condition. Cell-free BALF from SITO-treated rats contained measurable IL-6 with both doses, but it was only statistically significant for the 5-mg treatment group and at early time-points (Fig. 3B). Both doses of VD-induced elevated IL-6 at the earlier time-points as well. For IL-1 β , all particles and doses induced elevated levels on day 1. BALF from rats treated with SITO and VD had persistently high IL-1 β out to 90 days post-exposure (Fig. 3C).

Assessment of BAL macrophage phagocytosis

Indium lung toxicity has been associated with PAP (Cummings *et al.*, 2010; Cummings *et al.*, 2012). Phagocytic dysfunction in macrophages is thought to be a cause of this build-up of surfactant and other proteins in the lung (Kitamura *et al.*, 1999; Greenhill and Kotton, 2009). To examine whether particle instillations affected the phagocytic ability of lavaged alveolar macrophages, an assay was employed to evaluate subsequent particle uptake outside of the lung. In this assay, phagocytic cells from BALF were plated (controlling for macrophage numbers) and exposed to pH-sensitive *E. coli* particles that fluoresce when properly phagocytosed. Macrophages isolated from 1-mg In₂O₃ rats on day 7 post-IT showed a slight but significant enhancement in average phagocytic ability compared to macrophages from rats exposed only to the vehicle control, but this effect was not observed at the higher dose ($130.3 \pm 15.3\%$ 1 mg vs. $73.7 \pm 7.8\%$ 5 mg In₂O₃, mean \pm SEM) (Fig. 4A).

In contrast, macrophages isolated from rat lungs 7 days post-treatment with SITO demonstrated a decrease in the average phagocytic ability at both doses ($49.1 \pm 1.1\%$, 1 mg and $19.1 \pm 1.4\%$, 5 mg SITO, mean \pm SEM) (Fig. 4A). This effect was as potent as pretreating a group of vehicle control cells with Cytochalasin D, a known inhibitor of phagocytosis. Similar to the SITO groups, macrophages from VD-treated rat lungs were very ineffective at *E. coli* particle phagocytosis 7 days post-IT ($36.6 \pm 2.1\%$, 0.5 mg and $11.1 \pm 1.9\%$, 1 mg VD, mean \pm SEM) (Fig. 4A). These effects appeared to resolve by 90 days post-IT. In fact, cells from day 90 1-mg VD rats had enhanced phagocytosis over controls ($146.3 \pm 9.0\%$ 1-mg VD, mean \pm SEM). This was the only significant difference noted at day 90.

Plasma indium concentrations

Current exposure assessment for workers handling indium-containing materials involves measuring blood indium concentrations. Whether or not this is an accurate predictor of current exposures or lung disease remains to be determined (Omae *et al.*, 2011; Liu *et al.*, 2012). Thus, an aim of our study was to evaluate indium in the plasma throughout the time-course. Plasma from rats treated with 1-mg In₂O₃ contained very little indium, whereas the

higher dose showed a time-dependent increase in indium concentration (Fig. 5). However, these values were still low (<2 mcg l^{-1}). Similarly, SITO induced increases in plasma indium over the time course, and this effect was more dramatic with the 5-mg dose. In fact, between days 1 and 90, 5-mg SITO-derived plasma indium concentrations increased 6.8-fold (12.5 ± 0.6 mcg ml^{-1} D1 vs. 85.3 ± 7.7 mcg l^{-1} D90 SITO, mean \pm SEM).

Interestingly, plasma indium from VD-treated rats displayed different kinetics compared with In_2O_3 and SITO, as it peaked on day 7 (Fig. 5). Whether concentrations were further elevated past day 7 but prior to day 90 is unknown, as plasma indium concentrations were not measured on days 8 to 89. It is also intriguing that 1-mg VD at day 7 caused plasma indium levels comparable to 5-mg SITO at day 90 (93.5 ± 19.2 mcg ml^{-1} 1-mg VD vs. 85.3 ± 7.7 mcg l^{-1} 5-mg SITO, mean \pm SEM). A possible explanation is the presence of different forms of indium on the surface of each particle type.

Pulmonary histopathology findings

Hematoxylin and eosin (H&E) and Picrosirius Red stained sections of lung from animals were evaluated microscopically for evidence of inflammation, alveolar proteinosis (PAP) and interstitial fibrosis 90 days post-exposure. The incidence and mean severity of the microscopic findings for each group are summarized in Table 1. The analysis was carried out primarily to determine the relative severity of the lesions among treatment groups. Chronic bronchiointerstitial pneumonia was seen in the lungs of all exposed animals examined. Histologically, these changes were characterized by the presence of increased numbers of macrophages admixed with fewer neutrophils within alveolar walls and alveolar spaces, often centered on terminal bronchioles. Other microscopic changes included prominent type II pneumocyte hypertrophy and hyperplasia (Fig. 6B), pleural inflammation and fibrosis, and variable amounts of alveolar exudation consistent with PAP (Fig. 6B, C). Interstitial fibrosis, seen as increased amounts of red-staining fibrillar collagen in Picrosirius Red-stained sections of lung, was frequently observed in exposed animals (Fig. 6E, F). Fibrotic changes tended to be most prominent in areas of inflammation and type II pneumocyte hyperplasia, suggesting deposition of collagen in response to pulmonary injury and repair.

The severity of fibrotic and inflammatory changes in the lung ranged from minimal to severe depending on the particle type and dose. Interestingly, proteinosis tended to be more severe in the lungs of animals exposed to 5 mg of SITO (Fig. 6C), despite the fact that the majority of these animals had mild pathology. Overall, the pathology was most severe in lungs of animals exposed to VD, despite exposure to a lower particle dose when compared with SITO or In_2O_3 .

Discussion

The increased use of indium-containing materials in manufacturing has caused concern for workers exposed to these particles in their occupational environment. In the last decade or so, there have been multiple case reports of workers in the ITO industry developing severe, sometimes fatal, lung disease. As the industry continues to expand, the pathogenesis of indium lung disease merits investigation.

Intratracheal instillation of ITO production particles in this study caused significant lung damage and inflammation. In general, particles containing sintered ITO (SITO and VD) were more toxic than the pure In_2O_3 particles. The reason for this is unclear, but our findings agree with previous pulmonary rat studies where ITO particles induced more inflammation and damage than In_2O_3 (Lison *et al.*, 2009; Nagano *et al.*, 2011a, b; Lim *et al.*, 2014). The damage and inflammation induced by In_2O_3 (according to BALF parameters) was delayed compared with the other two particle types. Although compositionally different, all three samples have In_2O_3 on their particle surfaces as previously characterized (Badding *et al.*, 2014b). Thus, the presence of In_2O_3 is likely not the sole pneumotoxic entity of these particles.

Indium salts, which are present on VD particles, are known to be significantly more soluble than In_2O_3 (A. Stefaniak, personal communication). This would make dissolution of indium ions from VD particles more rapid than the other particle types. The enhanced solubility of this form of indium from VD may influence the toxic effects seen in our study. Besides being used at a lower dose (0.5 mg), VD particles also contain less total surface indium on a per mass basis (12% VD versus 24% for SITO) and yet are equally, if not more, toxic to rat lungs. This further enhances the suggestion that greater indium solubility may influence particle toxicity. Gwinn *et al.* (2015) recently demonstrated that solubilization of ionic indium from particles engulfed by macrophages correlated with *in vitro* macrophage cytotoxicity and *in vivo* pulmonary toxicity. Specifically, they showed that soluble InCl_3 (an indium salt) caused much greater cytotoxicity in cultured macrophages than less soluble forms of indium.

Measurements of indium in the blood plasma suggest that some of the metal did, in fact, move out of the lung. One scenario in which this may have occurred is the release of indium ions from particles within the lung to the blood. Another could be extravasation of particles from the lung due to tissue injury, which then release indium outside of the lung. Other studies have revealed indium elimination from the lung and distribution throughout the blood and lymph nodes (Nagano *et al.*, 2011a, b) and other organs such as the spleen, liver, brain (Lim *et al.*, 2014) after ITO pulmonary exposures. Two studies by Nagano *et al.* (2011a, b) showed that 13-week inhalation exposures in both rats and mice led to higher blood indium concentrations with ITO compared with In_2O_3 , which our findings in Fig. 5 confirm. Plasma indium was highest at 7 days post-IT for VD, as opposed to 90 days with In_2O_3 and SITO. Given that we only measured blood indium at three-time points (and none between 7 and 90 days), the peaks may have been different for these samples. However, in general, indium dissolution from VD particles appeared to occur more rapidly than the other particle types. Whether this is indicative of more severe pulmonary damage and overall toxicity as a biomarker is unknown, but the plasma indium concentrations seemed to correlate with the extent and timing of pulmonary damage and inflammatory cell infiltrates. For example, plasma indium was highest when LDH and cells in BALF were highest (at day 7 for VD vs. day 90 for SITO and In_2O_3) (Figs. 1 and 5).

BALF parameters for rats treated with In_2O_3 or SITO revealed increasing, and persistent elevations in LDH and inflammatory cell infiltrates over a 90-day time course; although this was less severe for In_2O_3 treatments (Fig. 1). In contrast, VD-treated rats showed a robust

initial increase in BALF parameters, followed by decreased LDH and recovered inflammatory cells at 90 days post-IT. These parameters were still significantly elevated compared to the vehicle controls, but less than the day 7 BALF findings. However, the cellularity seen with histology in day 90 VD-treated rats (Fig. 6B) suggests that inflammation persisted in the lungs with these treatments. In cases where alveoli contain activated macrophages, such as what was seen in animals exposed to VD, these macrophages are large and stick to alveolar walls and are not easily removed from the lung with BAL. This phenomenon has been observed in previous studies, resulting in fewer cells recovered from lavage (Porter *et al.*, 2007).

The comparisons among particle types are flawed by the fact that the high dose of VD was 1 mg versus 5 mg for In₂O₃ and SITO. However, if we just compare the 1-mg BALF results, VD-induced more LDH release into BALF than the other particle types at day 7 (Fig. 1A). Although, there was no difference in cell counts between 1 mg treatments of SITO or VD at this time point. By day 90, LDH in the 1 mg SITO rat BALF was higher than the 1 mg VD group, and total recovered cells in the 1 mg SITO exceeded that of VD. Thus, it is difficult to say whether SITO or VD was more overtly toxic to the rats' lungs at a 1 mg dose by strictly examining the BALF.

Cytokines are another indicator of inflammation in the lungs of treated rats. Figure 3 further demonstrates the presence of a proinflammatory response by SITO and VD exposures. Elevated IL-6 and IL-1 β in the BALF of SITO and VD-treated rats may be initiating factors in the development of fibrotic lesions (seen in day 90 lungs). Strong clinical evidence has implicated IL-6 in fibrosis development, as patients with idiopathic pulmonary fibrosis have elevated IL-6 in their BALF (Jones *et al.*, 1991; Takizawa *et al.*, 1997). A study utilizing an IL-1 receptor antagonist in mice treated with bleomycin or silica demonstrated the strong influence of this cytokine in lung fibrogenesis (Piguet *et al.*, 1993). Another study used gene transfer to overexpress IL-1 β in rat lungs to elicit a pro-fibrotic response (Kolb *et al.*, 2001). Thus, our histopathological findings of fibrosis in regions of lung inflammation (Fig. 6) suggest that a long-term consequence of ITO exposure-induced cytokine release, and inflammation is scarring. Similarly, clinical cases of workers in the ITO industry have revealed that pulmonary fibrosis sometimes occurs as a result of indium-containing particle exposures (Cummings *et al.*, 2012). Further, a recent study from our lab demonstrated the ability of SITO and VD to induce inflammasome activation and subsequent IL-1 β release from macrophages *in vitro* (Badding *et al.*, 2015). Here, the cytokine measurements from rat BALF confirm that IL-1 β release occurs *in vivo* as well (Fig. 3C).

One of the most intriguing findings was the altered phagocytic ability of pulmonary phagocytes isolated from rats treated with SITO or VD particles in Fig. 4. Whether the decrease was due to macrophage impairment (possibly in response to particle overload) or a change in the mononuclear cell population recovered in the BALF is unclear. Under conditions of pulmonary inflammation, some monocyte phenotypes can have lower phagocytic activity than normal resident alveolar macrophages (Brittan *et al.*, 2014). Thus, the influx and/or proliferation of macrophage populations within the lung following particle exposures may have differential effects on subsequent pathogen uptake. We previously used this same assay to show that pre-uptake of SITO or VD caused reduced *E. coli* phagocytosis

in the transformed mouse macrophage cell line, RAW 264.7 (Badding *et al.*, 2015). A clinical outcome of indium compound exposure in ITO workers is PAP, which is thought to be as a result of macrophage dysfunction (Kitamura *et al.*, 1999; Greenhill and Kotton, 2009). Therefore, the implications of our results are that cellular uptake of indium-containing particles may lead to the altered phagocytic function of lung macrophages, leading to excess surfactant. These results suggest a potential mechanism for PAP pathogenesis in ITO workers. Whether these exposures lead to increased susceptibility of workers to pulmonary infections is not known, but may deserve further investigation.

Signs of PAP, such as alveoli filled with lipoprotein material, were evident in the lungs of animals treated with all three particle types. The mean severity of PAP was greater than fibrosis in animals treated with SITO (PAP: 4.3 vs. fibrosis: 3.3, 5 mg SITO), whereas these two endpoints were roughly the same for animals treated with In₂O₃ (e.g. PAP: 3 vs. fibrosis: 3.2, 5 mg In₂O₃). In workers with indium lung disease, PAP tends to develop prior to fibrosis (within 6–14 months of hire for PAP vs. 2–14 years of hire for fibrosis) (Cummings *et al.*, 2012). This has been seen in other rat studies as well (Nagano *et al.*, 2011a, b). Thus, early damage and inflammation seemed to induce fibrotic changes, which indicate long-term consequences of an initial bolus exposure.

In general, the present study demonstrated that particles generated during the grinding of SITO tiles and the reclamation of indium (VD) were toxic to rat lungs. This was reflected in pulmonary changes involving significant inflammation, alveolar protein accumulation, and scarring. These changes have also been seen in case studies of workers in the ITO industry who develop indium lung disease. Our findings here and in a previous study suggest that altered phagocyte function following particle exposures may play a role in the pathogenesis of indium lung disease. With ITO production on the rise, workers who handle indium-containing particles should be monitored for changes in lung health and blood indium.

Acknowledgments

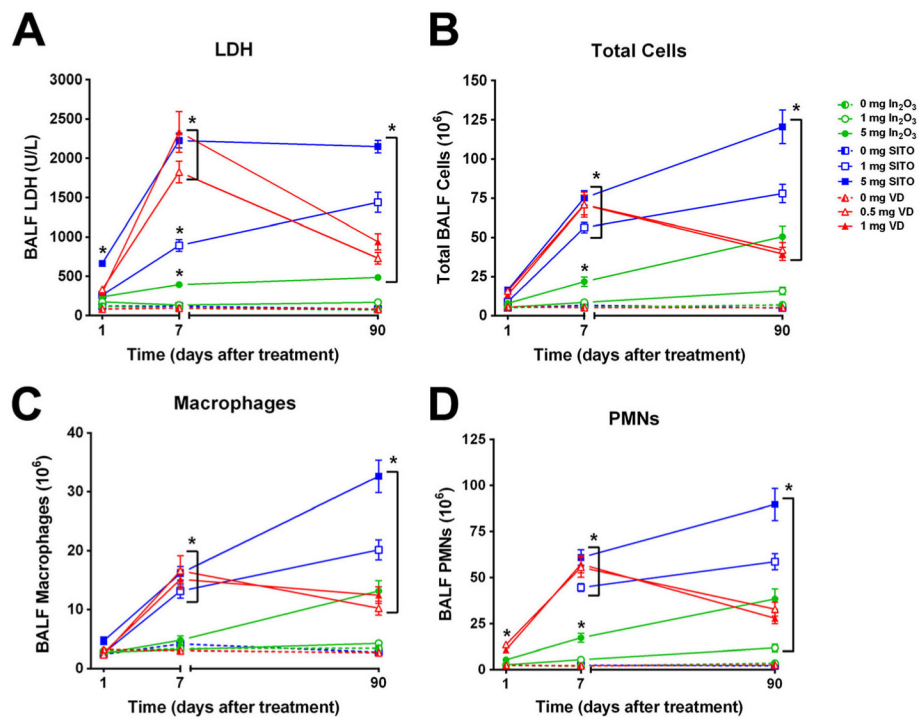
We would like to thank the pathology core at the National Institute for Occupational Safety and Health (NIOSH) for their technical assistance in preparing tissue slides.

References

- Antonini JM, Yang HM, Ma JY, Roberts JR, Barger MW, Butterworth L, Charron TG, Castranova V. Subchronic silica exposure enhances respiratory defense mechanisms and the pulmonary clearance of *Listeria monocytogenes* in rats. *Inhal Toxicol.* 2000; 12:1017–1036. [PubMed: 11015141]
- Badding MA, Fix NR, Antonini JM, Leonard SS. A comparison of cytotoxicity and oxidative stress from welding fumes generated with a new nickel-, copper-based consumable versus mild and stainless steel-based welding in RAW 264.7 mouse macrophages. *PLoS One.* 2014a; 9:e101310. [PubMed: 24977413]
- Badding MA, Schwegler-Berry D, Park JH, Fix NR, Cummings KJ, Leonard SS. Sintered indium-tin oxide particles induce pro-inflammatory responses in vitro, in part through inflammasome activation. *PLoS One.* 2015; 10:e0124368. [PubMed: 25874458]
- Badding MA, Stefaniak AB, Fix NR, Cummings KJ, Leonard SS. Cytotoxicity and characterization of particles collected from an indium–tin oxide production facility. *J Toxicol Environ Health A.* 2014b; 77:1193–1209. [PubMed: 25208660]

- Brittan M, Barr LC, Anderson N, Morris AC, Duffin R, Marwick JA, Rossi F, Johnson S, Dhaliwal K, Hirani N, Rossi AG, Simpson AJ. Functional characterisation of human pulmonary monocyte-like cells in lipopolysaccharide-mediated acute lung inflammation. *J Inflamm (Lond)*. 2014; 11 eCollection 2014. 10.1186/1476-9255-11-9
- Chonan T, Taguchi O, Omae K. Interstitial pulmonary disorders in indium-processing workers. *Eur Resp J*. 2007; 29:317–324.
- Cummings KJ, Donat WE, Ettensohn DB, Roggli VL, Ingram P, Kreiss K. Pulmonary alveolar proteinosis in workers at an indium processing facility. *Am J Respir Crit Care Med*. 2010; 181:458–464. [PubMed: 20019344]
- Cummings KJ, Nakano M, Omae K, Takeuchi K, Chonan T, Y-I X, Harley RA, Roggli VL, Hebisawa A, Tallaksen RJ, Trapnell BC, Day GA, Saito R, Stanton ML, Suarathana E, Kreiss K. Indium lung disease. *Chest*. 2012; 141:1512–1521. [PubMed: 22207675]
- Cummings KJ, Suarathana E, Edwards N, Liang X, Stanton ML, Day GA, Saito R, Kreiss K. Serial evaluations at an indium-tin oxide production facility. *Am J Ind Med*. 2013; 56:300–307. [PubMed: 23109040]
- Cummings KJ, Virji MA, Trapnell BC, Carey B, Healey T, Kreiss K. Early changes in clinical, functional, and laboratory biomarkers in workers at risk of indium lung disease. *Ann Am Thorac Soc*. 2014; 11:1395–1403. [PubMed: 25295756]
- Greenhill SR, Kotton DN. Pulmonary alveolar proteinosis: A bench-to-bedside story of granulocyte-macrophage colony-stimulating factor dysfunction. *Chest*. 2009; 136:571–577. [PubMed: 19666756]
- Gwinn WM, Qu W, Bousquet RW, Price H, Shines CJ, Taylor GJ, Waalkes MP, Morgan DL. Macrophage solubilization and cytotoxicity of indium-containing particles as in vitro correlates to pulmonary toxicity in vivo. *Toxicol Sci*. 2015; 144:17–26. [PubMed: 25527823]
- Gwinn WM, Qu W, Shines CJ, Bousquet RW, Taylor GJ, Waalkes MP, Morgan DL. Macrophage solubilization and cytotoxicity of indium-containing particles in vitro. *Toxicol Sci*. 2013; 135:414–424. [PubMed: 23872580]
- Hamaguchi T, Omae K, Takebayashi T, Kikuchi Y, Yoshioka N, Nishiwaki Y, Tanaka A, Hirata M, Taguchi O, Chonan T. Exposure to hardly soluble indium compounds in ITO production and recycling plants is a new risk for interstitial lung damage. *Occup Environ Med*. 2008; 65:51–55. [PubMed: 17626138]
- Homma T, Ueno T, Sekizawa K, Tanaka A, Hirata M. Interstitial pneumonia developed in a worker dealing with particles containing indium-tin oxide. *J Occup Health*. 2003; 45:137–139. [PubMed: 14646287]
- Jones KP, Reynolds SP, Capper SJ, Kalinka S, Edwards JH, Davies BH. Measurement of interleukin-6 in bronchoalveolar lavage fluid by radio-immunoassay: Differences between patients with interstitial lung disease and control subjects. *Clin Exp Immunol*. 1991; 83:30–34. [PubMed: 1988228]
- Kim B-C, Lee J-H, Kim J-J, Ikegami T. Rapid rate sintering of nanocrystalline indium tin oxide ceramics: Particle size effect. *Mater Lett*. 2002; 52:114–119.
- Kitamura T, Tanaka N, Watanabe J, Uchida KS, Yamada Y, Nakata K. Idiopathic pulmonary alveolar proteinosis as an autoimmune disease with neutralizing antibody against granulocyte/macrophage colony-stimulating factor. *J Exp Med*. 1999; 190:875–880. [PubMed: 10499925]
- Kolb M, Margetts PJ, Anthony DC, Pitossi F, Gauldie J. Transient expression of IL-1 β induces acute lung injury and chronic repair leading to pulmonary fibrosis. *J Clin Invest*. 2001; 107:1529–1536. [PubMed: 11413160]
- Lim CH, Han J-H, Cho H-W, Kang M. Studies on the toxicity and distribution of indium compounds according to particle size in Sprague–Dawley rats. *Toxicol Res*. 2014; 30:55–63. [PubMed: 24795801]
- Lison D, Laloy J, Corazzari I, Muller J, Rabolli V, Panin N, Huaux F, Fenoglio I, Fubini B. Sintered indium-tin-oxide (ITO) particles: A new pneumotoxic entity. *Toxicol Sci*. 2009; 108:472–481. [PubMed: 19176593]

- Liu HH, Chen CY, Chen GI, Lee LH, Chen HL. Relationship between indium exposure and oxidative damage in workers in indium tin oxide production plants. *Int Arch Occup Environ Health*. 2012; 85:447–453. [PubMed: 21833746]
- Mann PC, Vahle J, Keenan CM, Baker JF, Bradley AE, Goodman DG, Harada T, Herbert R, Kaufmann W, Kellner R, Nolte T, Rittinghausen S, Tanaka T. International harmonization of toxicologic pathology nomenclature: An overview and review of basic principles. *Toxicol Path*. 2012; 40:7S–13S. [PubMed: 22637736]
- Nagano K, Gotoh K, Kasai T, Aiso S, Nishizawa T, Ohnishi M, Ikawa N, Eitaki Y, Yamada K, Arito H, Fukushima S. Two- and 13-week inhalation toxicities of indium-tin oxide and indium oxide in rats. *J Occup Health*. 2011a; 53:51–63. [PubMed: 21233592]
- Nagano K, Nishizawa T, Eitaki Y, Ohnishi M, Noguchi T, Arito H, Fukushima S. Pulmonary toxicity in mice by 2- and 13-week inhalation exposures to indium-tin oxide and indium oxide aerosols. *J Occup Health*. 2011b; 53:234–239. [PubMed: 21422720]
- Nakano M, Omae K, Tanaka A, Hirata M, Michikawa T, Kikuchi Y, Yoshioka N, Nishiwaki Y, Chonan T. Causal relationship between indium compound inhalation and effects on the lungs. *J Occup Health*. 2009; 51:513–521. [PubMed: 19834281]
- NIOSH. Hazard Evaluation and Technical Assistance Report: An Evaluation of Preventive Measures at an Indium-Tin Oxide Production Facility. Morgantown, WV: U.S. Department of Health and Human Services, Public Health Service, Centers for Disease Control and Prevention; 2012. Publication No. HETA 2009-0214-3153
- Omae K, Nakano M, Tanaka A, Hirata M, Hamaguchi T, Chonan T. Indium lung--case reports and epidemiology. *Int Arch Occup Environ Health*. 2011; 84:471–477. [PubMed: 20886351]
- Piguet PF, Vesin C, Grau GE, Thompson RC. Interleukin 1 receptor antagonist (IL-1ra) prevents or cures pulmonary fibrosis elicited in mice by bleomycin or silica. *Cytokine*. 1993; 5:57–61. [PubMed: 7683505]
- Porter DW, Hubbs AF, Baron PA, Millecchia LL, Wolfarth MG, Battelli LA, Schwegler-Berry DE, Beighley CM, Andrew ME, Castranova V. Pulmonary toxicity of Expancel microspheres in the rat. *Toxicol Path*. 2007; 35:702–714. [PubMed: 17763284]
- Shackelford C, Long G, Wolf J, Okerberg C, Herbert R. Qualitative and quantitative analysis of nonneoplastic lesions in toxicology studies. *Toxicol Path*. 2002; 30:93–96. [PubMed: 11890482]
- Takizawa H, Satoh M, Okazaki H, Matsuzaki G, Suzuki N, Ishii A, Suko M, Okudaira H, Morita Y, Ito K. Increased IL-6 and IL-8 in bronchoalveolar lavage fluids (BALF) from patients with sarcoidosis: Correlation with the clinical parameters. *Clin Exp Immunol*. 1997; 107:175–181. [PubMed: 9010273]
- Tanaka A, Hirata M, Homma T, Kiyohara Y. Chronic pulmonary toxicity study of indium-tin oxide and indium oxide following intratracheal instillations into the lungs of hamsters. *J Occup Health*. 2010; 52:14–22. [PubMed: 19940388]
- Udawatte CP, Yanagisawa K. Fabrication of low-porosity indium tin oxide ceramics in air from hydrothermally prepared powder. *J Am Ceramic Soc*. 2001; 84:251–253.

**Figure 1.**

Lactate dehydrogenase (LDH) levels and inflammatory cell counts in rat bronchoalveolar lavage fluid (BALF) over a time course of 90 days post-exposure. (A) LDH concentration in BALF from days 1, 7, and 90 post-IT of particle suspensions. In₂O₃ (circles), SITO (squares), and VD (triangles) symbols represent the mean \pm SEM ($n = 6-8$ rats). From the same BALF, (B) total cells, (C) macrophages and (D) PMNs were counted. (Note: PMNs were not counted on day 1 for SITO). * $P < 0.05$ compared with phosphate-buffered saline (PBS) vehicle controls (0 mg) on that day.

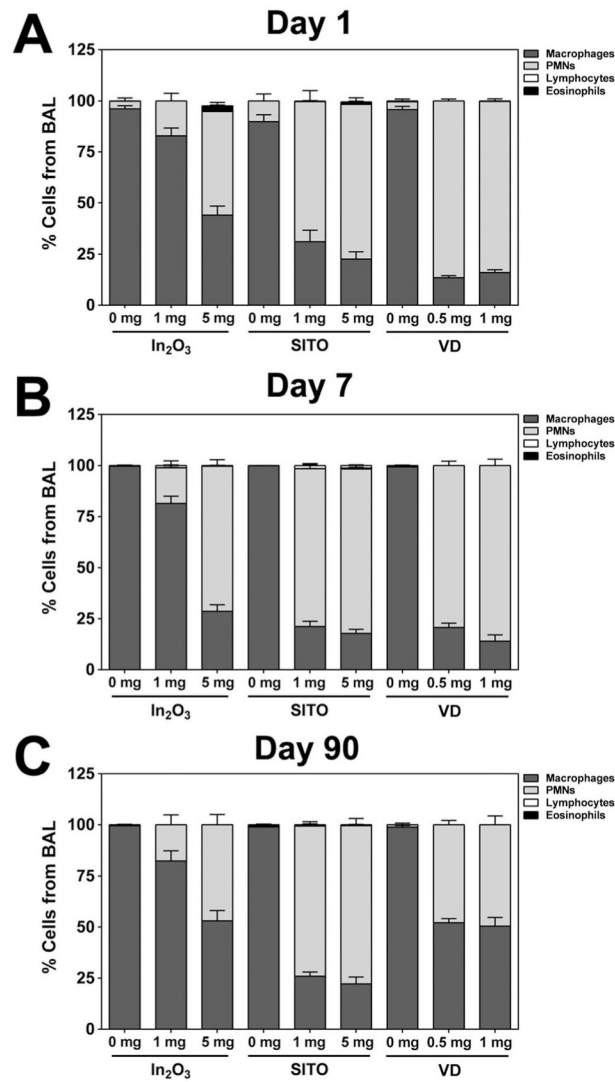


Figure 2. Cell differentials from bronchoalveolar lavage fluid (BALF) over a time course of exposure. Cells from (A) day 1, (B) day 7 and (C) day 90 rats were designated as macrophages, PMNs, lymphocytes, or eosinophils ($200 \text{ cells rat}^{-1}$). The percentage of cells scored as each cell type was calculated, and bars represent the mean percentage \pm SEM ($n = 6-8$ rats).

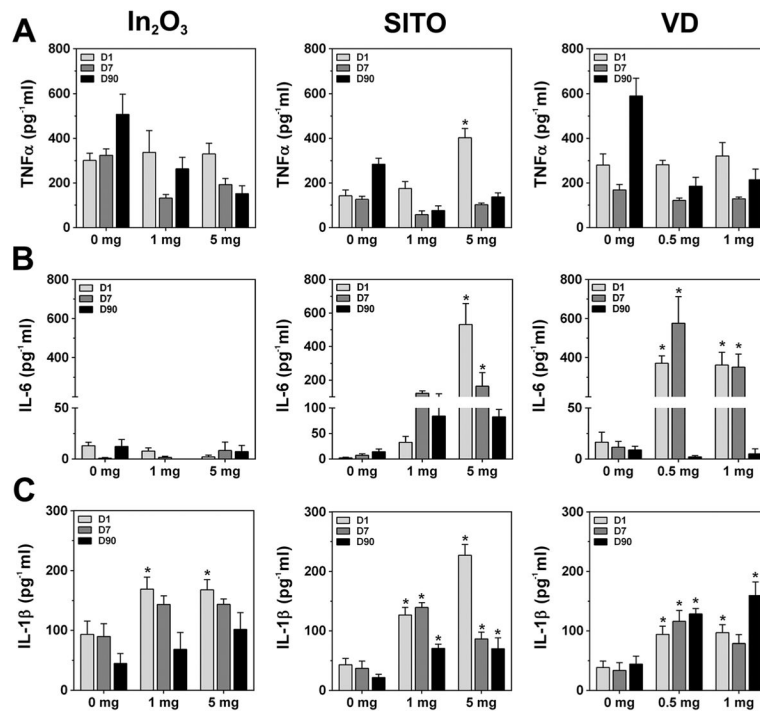


Figure 3. Cytokine concentrations in bronchoalveolar lavage fluid (BALF). Concentrations of (A) TNF- α , (B) IL-6 and (C) IL-1 β were measured in BALF from In₂O₃, SITO and VD-treated rats. * $P < 0.05$ compared with the 0 mg controls on that day.

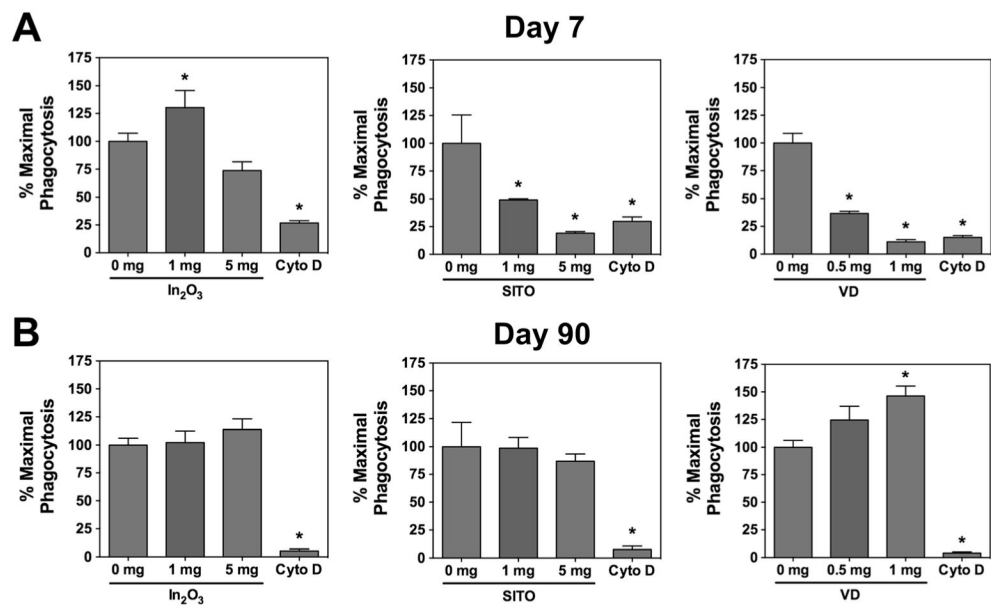


Figure 4.

Phagocytosis of *Escherichia coli* by bronchoalveolar lavage fluid (BALF) phagocytes. Cells from the BALF of (A) day 7 or (B) day 90 rats were plated at 2×10^5 macrophages/well, washed to remove unattached cells, and treated with pHrodo™ Red *E. coli* BioParticles® for 2 h to allow phagocytosis. A separate set of plated control cells (0 mg) received Cytochalasin D (Cyto D) to prevent phagocytosis. Plates were read to measure changes in fluorescence, and values were normalized to the phosphate-buffered saline (PBS) controls (0 mg) to represent maximal phagocytosis. Error bars represent the mean \pm SEM ($n = 4-5$ rats). * $P < 0.05$ compared with 0-mg controls.

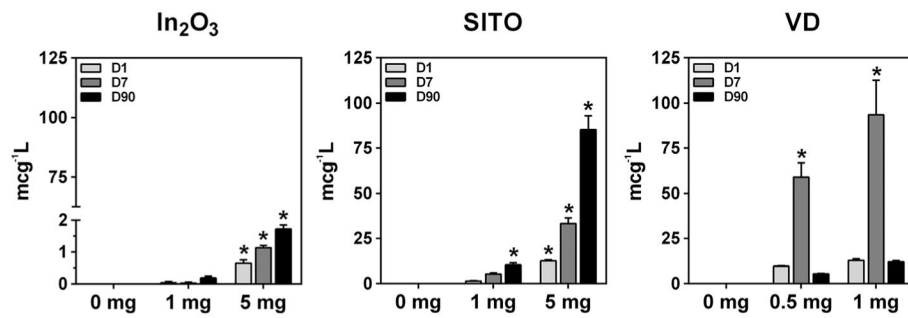


Figure 5. Plasma indium concentrations over a time-course. Whole blood was collected from rats, and plasma indium content measured using inductively coupled plasma mass spectrometry (ICP-MS). Error bars represent the mean \pm SEM ($n = 4$ rats). * $P < 0.05$ compared with 0-mg controls.

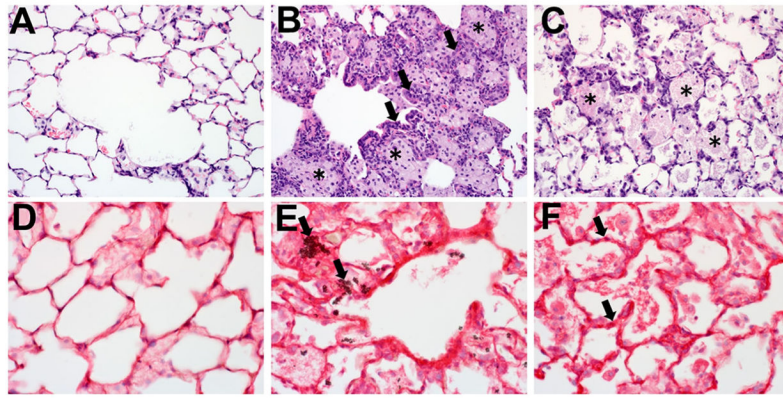


Figure 6.

Histopathological findings in rat lungs 90 days post-IT. Lung sections from day 90 rats were stained with Hematoxylin and eosin (H&E) and Picrosirius Red and evaluated for inflammation, fibrosis and alveolar proteinosis. (A) Photomicrograph of H&E stained section of lung from a control animal (200 x magnification). (B) Lung from an animal exposed to 0.5-mg VD showing alveoli filled with foamy macrophages (asterisk) and alveolar walls lined by hyperplastic type II pneumocytes (arrows) (200 x magnification). (C) Alveoli containing abundant eosinophilic material consistent with lipoprotein (asterisk) from animal exposed to 5-mg SITO (200 x magnification). (D) Photomicrograph of Picrosirius red stained section of lung from a control animal showing normal pattern of collagen staining in alveolar walls (400 x magnification). (E) Increased interstitial collagen observed in alveolar walls, associated with deposition of particles (arrows) from an animal treated with 5 mg of In_2O_3 (400 x magnification). (F) Lung from an animal exposed to 1 mg of VD. Alveolar walls are thickened by fibrosis (arrows) (400 x magnification).

Histopathology analysis of lung inflammation and fibrosis

Table 1

	In ₂ O ₃			SITO			VD		
	0 mg	1 mg	5 mg	0 mg	1 mg	5 mg	0 mg	0.5 mg	1 mg
Number of rats	5	5	5	3	3	3	3	3	5
Inflammation incidence (mean severity score)	2(1)	5(1.8)	5(2.8)	1(1)	3(2)	3(2.3)	2(1.5)	3(3.3)	5(3.4)
Alveolar proteinosis (mean severity score)	0(0)	1(1)	5(3)	0(0)	3(2.7)	3(4.3)	0(0)	3(3.3)	5(3.8)
Fibrosis incidence (mean severity score)	0(0)	2(1)	5(3.2)	0(0)	3(2)	3(3.3)	0(0)	3(3.6)	5(4)

For each exposure group, the mean severity scores () were calculated by determining the sum of the group severity scores divided by the number of animals affected.